

Marquette University  
**e-Publications@Marquette**

---

Chemistry Faculty Research and Publications

Chemistry, Department of

---

1-1-2005

# The Effects Of Triphenylphosphate and Recorcinolbis(Diphenylphosphate) on the Thermal Degradation Of Polycarbonate in Air

Bok Nam Jang  
*Marquette University*

Charles A. Wilkie  
*Marquette University*, [charles.wilkie@marquette.edu](mailto:charles.wilkie@marquette.edu)

---

Accepted version. *Thermochimica Acta*, Volume 433, Issues 1-2, pp 1-12 (August, 2005). DOI: © 2005 Elsevier B.V. Used with permission.

Marquette University

e-Publications@Marquette

***Chemistry Faculty Research and Publications/College of Arts and Sciences***

***This paper is NOT THE PUBLISHED VERSION; but the author's final, peer-reviewed manuscript.*** The published version may be accessed by following the link in the citation below.

*Thermochimica Acta*, Vol. 433, No. 1-2 (August 2005): 1-12. [DOI](#). This article is © Elsevier and permission has been granted for this version to appear in [e-Publications@Marquette](#). Elsevier does not grant permission for this article to be further copied/distributed or hosted elsewhere without the express permission from Elsevier.

# The Effects Of Triphenylphosphate And Resorcinolbis(Diphenylphosphate) On The Thermal Degradation Of Polycarbonate In Air

Bok Nam Jang

Department of Chemistry, Marquette University, Milwaukee, WI

Charles A. Wilkie

Department of Chemistry, Marquette University, Milwaukee, WI

## Abstract

The thermal degradation of polycarbonate/triphenylphosphate (PC/TPP) and PC/resorcinolbis(diphenylphosphate) (PC/RDP) in air has been studied using TGA/FTIR and GC/MS. In PC/phosphate blends, the phosphate stabilizes the carbonate group of polycarbonate from alcoholysis between the alcohol products of polycarbonate degradation and the carbonate linkage. Thus, the evolution of bisphenol A, which is mainly produced via hydrolysis/alcoholysis of the carbonate linkage, is significantly reduced, while, the evolution of various alkylphenols and diarylcarbonates increases. The bonds that are broken first in the thermal degradation of both the carbonate and isopropylidene linkages of polycarbonate are the weakest bonds in each, when a phosphate is present. Triphenylphosphate and resorcinolbis(diphenyl-phosphate), even though they exhibit a significant difference in their volatilization temperature, appear to play a similar role in the degradation pathway of polycarbonate.

## Keywords

Polycarbonate, Thermal degradation, Fire retardancy, Triphenylphosphate, Resorcinoldiphosphate

## 1. Introduction

Since the environmental issues of halogen compounds were raised in the 1980s, halogen fire retardants have been voluntarily phased out, especially in the European market, and non-halogenated fire retardant systems have been very actively studied and used [\[1\]](#), [\[2\]](#). Among non-halogenated fire retardants, aryl-phosphates are representative, because they are generally thermally stable and exhibit good plasticization and compatibility with many polymers. However, there are only a few non-halogenated fire retardant polymer systems using aryl-phosphates as flame retardants [\[2\]](#), [\[3\]](#), [\[4\]](#).

The aryl-phosphates include monophosphates, such as triphenylphosphate (TPP), tricresylphosphate, cresyldiphenyl phosphate, trixylylphosphate, etc., and bisphosphates including resorcinol bis(diphenylphosphate) (RDP), bisphenol A bis(diphenylphosphate), etc. Both condensed phase and vapor phase fire retardant effects have been suggested as the modes of action for the aryl-phosphates [\[5\]](#), [\[6\]](#), [\[7\]](#), [\[8\]](#). The vapor phase fire retardation effect is considered to be identical to the radical trap mechanism of halogen compounds, capturing the hydrogen and hydroxy radicals which contribute to combustion reactions [\[11\]](#). The condensed phase mechanisms are mainly explained by coating and charring. Regarding the coating mechanism, it was suggested that phosphorus compounds could migrate to the surface, decompose to phosphoric acid and these acids could form a molten viscous surface layer protecting the polymer substrate from flame and oxygen [\[14\]](#). For the charring mechanism, it was felt that aryl-phosphates promote and enhance char formation.

Among aryl-phosphates, TPP and RDP are very good examples for the study of degradation mechanisms, since they have relatively simple structures and show significantly different thermal mass loss behavior. Shank and co-workers studied the flame retardant mechanism for phosphorus flame retardancy of TPP in PPO/HIPS and suggested a predominantly vapor phase mechanism [\[9\]](#). Levchik and co-workers studied the thermal degradation of PPO/HIPS/RDP and PC/ABS/RDP using TGA and FTIR and proposed that RDP chemically reacts with PPO or PC and the fire retardant action is mainly a condensed phase mechanism [\[10\]](#), [\[11\]](#), [\[12\]](#). Although the fire retardant mechanisms of aryl-phosphates in the condensed phase were proposed in the above work, the mechanism of fire retardation by phosphorus compounds has not been elucidated in terms of reactions which occur and the products that result.

An accurate understanding of the mechanism of fire retardancy with a given polymer is very important in the design of more effective fire retardant systems and the fire retardant action is closely related to the degradation behavior of the polymer. In order to elucidate the fire retardant action of aryl-phosphates in polymer/aryl-phosphate blends, an understanding of the degradation pathway of the polymer is necessary. Polycarbonate (PC) is one of good char forming polymers and polycarbonate and its blend with acrylonitrile–butadiene–styrene (ABS) using aryl-phosphate fire retardants are widely used in electrical appliances.

Polycarbonate exhibits excellent mechanical properties and a high limiting oxygen index (LOI) value of 27 and produces a large fraction of char upon combustion [\[13\]](#). Thus, the thermal degradation of polycarbonate has been the subject of a number of studies. Lee [\[14\]](#) and McNeill and Rincon [\[15\]](#), [\[16\]](#) suggested homolytic chain scission mechanisms on the thermal degradation of PC. Davis and Golden proposed the Kolbe–Schmitt rearrangement of carbonate linkage for the formation of xanthone structure [\[17\]](#), [\[18\]](#). Montaudo and co-workers assigned xanthone units as one of main evolved functional group and proposed that the major degradation pathway for PC is ester exchange of the carbonate linkage and disproportionation of isopropylidene linkage [\[19\]](#), [\[20\]](#), [\[21\]](#), [\[22\]](#), [\[23\]](#), [\[24\]](#). They also analyzed the THF-soluble fraction of thermally oxidized PC at 300 and 350 °C, and suggested that the

oxidation pathway begins with radical formation in the isopropylidene linkage through hydrogen cleavage, followed by subsequent rearrangement and peroxide formation [25].

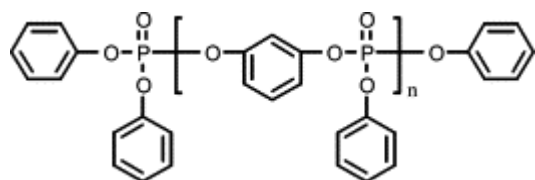
However, the environment of a decomposing sample may affect the degradation pathways. For instance, the degradation behavior upon heating and/or combustion may be altered in the presence of oxygen and the pressure during decomposition affects the composition of the evolved products. Since the above results were mostly acquired under vacuum or in an inert atmosphere, there are still some aspects of the degradation behavior during burning of polymers which require further elucidation. In this laboratory, TGA was used to study the thermal degradation of PC in nitrogen and air, to obtain information at atmospheric pressure as well as under real combustion conditions, and the significant evolved products were assigned using FTIR, GC/MS and LC/MS. It was proposed that the evolved products are produced mainly by chain scission of the isopropylidene linkage and hydrolysis/alcoholysis of the carbonate linkage, and that the presence of oxygen primarily affects only the beginning stage of degradation [26], [27].

In order to determine the effect of typical fire retardants on the degradation of polycarbonate, TPP and RDP were blended with PC at 12 wt.%, which is sufficient to obtain a UL94 V-0 rating [10], [11]. Since the burning of polymers is a very complicated thermal process and the heat and mass transfer through the burning surface of polymer substrate causes a large temperature gradient in the interior of the polymer, flash pyrolysis as well as gradual pyrolysis has been carried out using TGA in air to simulate real combustion. For the molecular structure identification, the evolved volatile products were analyzed using in situ vapor phase FTIR and the volatiles were also collected under each pyrolysis condition for further analysis using FTIR and GC/MS. The solid residues after pyrolysis were analyzed using FTIR.

## 2. Experimental

### 2.1. Materials

The polycarbonate sample was provided by Cheil Industries Inc., and was used as received; this material is end-capped with *t*-butyl phenol for enhanced thermal stability. The number and weight average molecular weight of the bisphenol A polycarbonate are 16,000 and 28,000, respectively. Triphenylphosphate (TPP) and resorcinolbis(diphenylphosphate) (RDP) were provided by Akzo Nobel and were also used as received. TPP is a white flake solid with a melting point of 48 °C, while, RDP contains 65% dimer ( $n = 1$ ), 30% higher oligomers ( $n \geq 2$ ) and up to 5% of TPP ( $n = 0$ ), as shown below.



### 2.2. Sample preparation

Polycarbonate and TPP or RDP were melt-blended in a Brabender Mixer for 5 min at 250 °C with 12 wt.% of phosphate in the total composition.

### 2.3. TGA/FTIR analysis

TGA/FTIR was carried out on a Cahn TG 131 instrument which was connected to a Mattson Research grade FTIR through stainless steel tubing. The temperature reproducibility of the TGA is  $\pm 3$  °C and error range of non-volatile fraction at 700 °C is  $\pm 3\%$ . The thermal degradation in TGA was carried out under an air flow of 80 ml/min. The sample size was 40–60 mg for the TGA evaluation. During thermal degradation in TGA, the evolved volatile products are introduced to the IR chamber through a sniffer tube and stainless steel tubing, and in situ vapor phase FTIR spectra are collected; this sniffer tube extends into the sample cup in TGA and removes the evolved products at the rate of 40 ml/min. The temperature of the tubing was 300 °C.

## 2.4. Gradual and flash pyrolysis and sampling of condensable evolved products

The heating rate of TGA/FTIR for the gradual pyrolysis was 20 °C/min. Flash pyrolysis was performed by placing the samples instantly at the specific temperature; the sample was placed in the sample cup and the furnace pre-heated to the desired temperature, then the furnace was moved up and closed within 5 s. The temperatures for the flash pyrolysis are 600 and 800 °C and vapor phase FTIR spectra are collected for the evolved volatile products at those temperatures. The condensable evolved products under each pyrolysis condition were sampled for 2–10 min as a function of mass loss using a cold trap at a temperature of –78 °C for further analysis.

## 2.5. Analysis of the condensable evolved products

The condensable products in gradual and flash pyrolysis were collected in a cold trap, and then dissolved in acetonitrile. FTIR (Nicolet Magna 560 Model) analysis was performed by placing the material on a KBr window and allowing the solvent to evaporate. GC/MS spectra were obtained using a Hewlett Packard 6850 series GC connected to a Hewlett Packard 5973 Series MS (70 eV electron ionization) with temperature programming from 40 to 250 °C. The structures of the evolved compounds were identified either by co-injection with authentic compounds to GC/MS or by the analysis of mass fragmentation pattern.

## 2.6. Analysis of solid residue sample

The solid residues were collected at each mass loss and analyzed by FTIR (Nicolet Magna Model 560) using KBr pellets.

# 3. Results and discussion

## 3.1. Gradual pyrolysis

### 3.1.1. Thermo gravimetric analysis (TGA) and in situ vapor phase FTIR

The TGA curves of TPP, RDP, PC, PC/TPP, and PC/RDP in air at a ramp rate of 20 °C/min are shown in [Fig. 1](#).

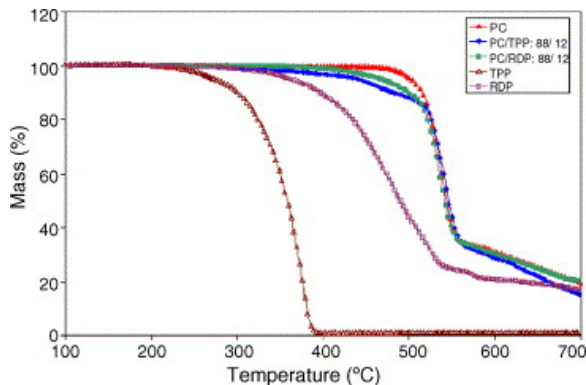


Fig. 1. TGA curves for the each composition at a heating rate of 20 °C per minute under an air atmosphere.

The mass loss temperatures of TPP and RDP are much lower than that of polycarbonate. In comparison with degradation of virgin polycarbonate (PC), since TPP and RDP are blended with PC, the mass loss onset temperatures of PC/TPP and PC/RDP are much lower than that of PC. The main mass loss region for both PC/TPP and PC/RDP ends at about 560 °C, as does virgin polycarbonate. Considering the mass percent of TPP and RDP in the composition, the solid residues for the blends are a little higher than expected. The solid residues at 560 °C show almost the same value, about 35%. As the degradation proceeds in air, the residue continues to degrade, eventually going to zero.

The in situ vapor phase FTIR spectra of the evolved volatile products of PC/TPP and PC/RDP at each mass loss are shown in [Fig. 2](#), [Fig. 3](#), respectively. CO<sub>2</sub> evolution at 2200–2400 cm<sup>-1</sup> and the weak noise-like bands at 1400–1900 and 3500–3900 cm<sup>-1</sup> due to H<sub>2</sub>O evolution were observed over the whole mass loss range. At the beginning of mass loss, the 5% mass loss spectra in [Fig. 2](#), [Fig. 3](#), mainly phosphates are evolved, because the

volatilization temperatures of TPP or RDP are low, as shown in [Fig. 1](#). The peaks at 1200 and 960  $\text{cm}^{-1}$  correspond to phosphorus–oxygen double bond stretching (P=O) and phosphorus–oxygen single bond stretching (P–O), respectively. Since the P=O stretching band is overlapped with the carbon–oxygen stretching region (1150–1300  $\text{cm}^{-1}$ ) of moieties, such as ethers, carbonates and phenols of evolved products of polycarbonate [\[28\]](#), the band at 960  $\text{cm}^{-1}$  is used as the diagnostic band for phosphates [\[11\]](#) [\[12\]](#). As the mass loss increases, the evolved products due to the polycarbonate degradation become more significant. The band due to alcohol at 3650  $\text{cm}^{-1}$  and the carbonyl band of carbonate at 1780  $\text{cm}^{-1}$  are observed in the 10% mass loss region, indicating that the polycarbonate degradation initiates and these bands become more significant at higher mass loss. Comparing the free alcohol band (3650  $\text{cm}^{-1}$ ) and phosphate band (960  $\text{cm}^{-1}$ ) at 10% mass loss of PC/TPP ([Fig. 2](#)) with that of PC/RDP ([Fig. 3](#)), a relatively intense alcohol band and weak phosphate band are observed in the presence of RDP. It appears that this result is due to the lower volatility of RDP, which means that the relatively strong alcohol band in PC/RDP in the low mass loss region, around 10% mass loss, is caused by some evolved products from the polycarbonate degradation.

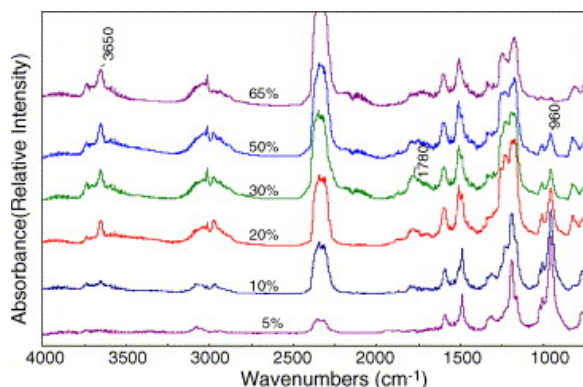


Fig. 2. In situ vapor phase FTIR for the polycarbonate/TPP blend (88/12). Inset percent denotes the mass loss where the IR spectrum is obtained.

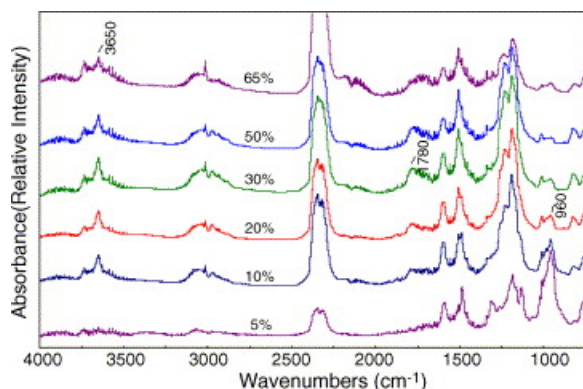


Fig. 3. In situ vapor phase FTIR for the polycarbonate/RDP blend (88/12). Inset percent denotes the mass loss where IR spectrum is obtained.

Considering the presence of 12 wt.% of TPP or RDP in the compositions and their ease of volatilization, it is notable that a trace of phosphate was detected in the evolved products at very high mass loss. The band at 960  $\text{cm}^{-1}$  can be observed up to 65% mass loss for both cases in the evolved volatile products. The results of vapor phase FTIR for PC/TPP and PC/RDP are almost identical in terms of functionality.

### 3.1.2. Analysis of condensable products evolved at each mass loss region

The evolved products of PC/TPP and PC/RDP were collected for each mass loss region and their FTIR spectra are shown in [Fig. 4](#), [Fig. 5](#), respectively. It is important to obtain the FTIR spectra for the condensable products, because some large molecules do not reach the IR chamber, due to their low volatility.

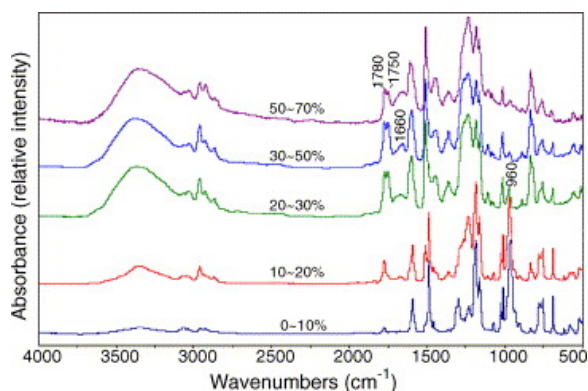


Fig. 4. FTIR of condensable evolved products of PC/TPP at each mass loss region.

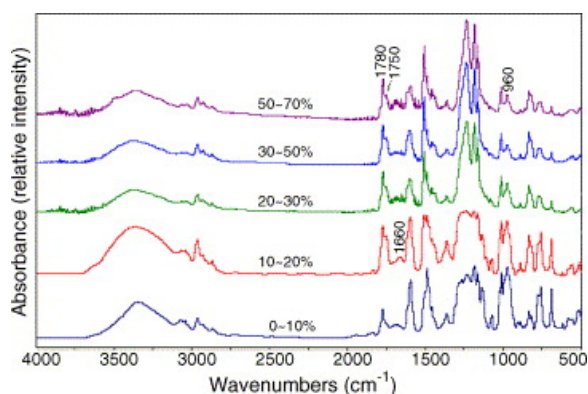


Fig. 5. FTIR of condensable evolved products of PC/RDP at each mass loss region.

Comparing the vapor phase spectra with those of the condensables, one can observe a stronger carbonate band, around 1750–1780 cm<sup>-1</sup>, and the presence of ketones, from a band near 1660 cm<sup>-1</sup> [27], [29]. These species must have a relatively low volatility, since they are not seen in significant intensity in the vapor phase spectrum, and they must arise from the degradation process. In the case of virgin polycarbonate degradation in air, the carbonate band was relatively small [27], however, for the PC/phosphates, the carbonate bands significantly increase, which suggests a considerable amount of carbonate evolution in the presence of phosphates. The relative intensity of ketone bands decrease, compared to the degradation of virgin polycarbonate in air. These results imply that phosphate may stabilize not only carbonate linkage, but also the isopropylidene linkage, from oxidative degradation.

In order to identify the structures of the evolved products, GC/MS was performed on the collected samples in each mass loss region of PC/TPP and PC/RDP, as shown in Fig. 6, Fig. 7. The GC trace has appended to it the *m/z* that have been discerned and the corresponding structures were identified, using the MS fragmentation patterns and functionality information from FTIR, and they are shown in Table 1, Table 2.

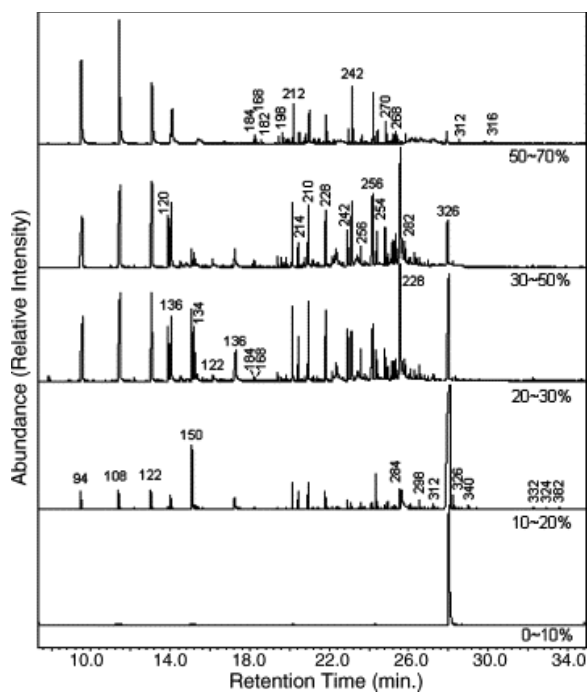


Fig. 6. GC traces for the condensable products of PC/TPP formulation at each mass loss. Inset numbers indicate the molecular weight acquired by mass spectroscopy.

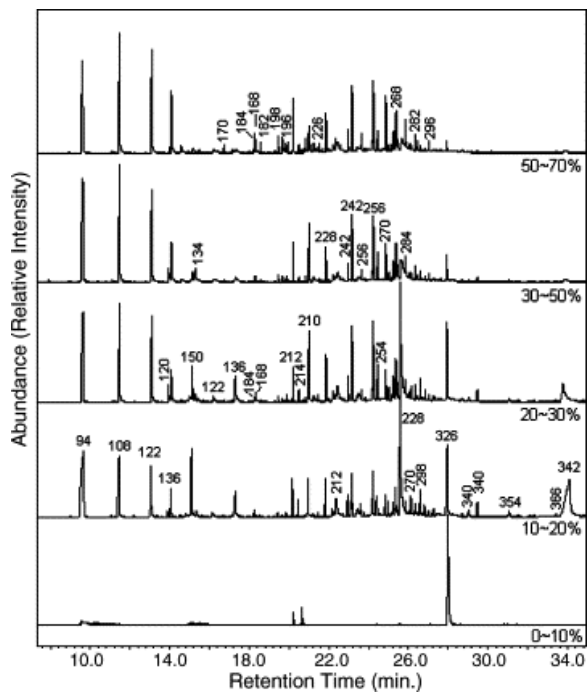


Fig. 7. GC traces for the evolved products of PC/RDP formulation at each mass loss. Inset numbers indicate the molecular weight acquired by mass spectroscopy.



Table 1. Assigned structures having one and two benzene rings from GC/MS results

Group	Structures ( <i>m/z</i> , retention time in minutes)
Alcohol	$\text{HO-C}_6\text{H}_5^+$ (94, 9.7), $\text{HO-C}_6\text{H}_4\text{-CH}_3^+$ (108, 11.6), $\text{HO-C}_6\text{H}_4\text{-C}_2\text{H}_5^+$ (122, 13.3), $\text{HO-C}_6\text{H}_4\text{-C}_2\text{H}_5^+$ (120, 13.8), $\text{HO-C}_6\text{H}_4\text{-C}_3\text{H}_7^+$ (136, 14.1), $\text{HO-C}_6\text{H}_4\text{-C}_4\text{H}_9^+$ (150, 15.0), $\text{HO-C}_6\text{H}_4\text{-C}_2\text{H}_5^+$ (134, 15.2), $\text{HO-C}_6\text{H}_4\text{-C}_6\text{H}_5^+$ (212, 22.3), $\text{HO-C}_6\text{H}_4\text{-C}_6\text{H}_4\text{-OH}^+$ (228, 25.6)
Aldehyde ketone	$\text{HO-C}_6\text{H}_4\text{-C(=O)-H}^+$ (122, 16.2), $\text{HO-C}_6\text{H}_4\text{-C(=O)-CH}_3^+$ (136, 17.2)
Furan	$\text{C}_6\text{H}_5\text{-O-C}_6\text{H}_5^+$ (168, 18.2), $\text{C}_6\text{H}_5\text{-O-C}_6\text{H}_4\text{-CH}_3^+$ (182, 18.6), $\text{C}_6\text{H}_5\text{-O-C}_6\text{H}_3\text{(CH}_3)_2^+$ (196, 19.7),
Ether	$\text{C}_6\text{H}_5\text{-O-C}_6\text{H}_5^+$ (170, 16.7), $\text{C}_6\text{H}_5\text{-O-C}_6\text{H}_4\text{-CH}_3^+$ (184, 18.3), $\text{C}_6\text{H}_5\text{-O-C}_6\text{H}_3\text{(CH}_3)_2^+$ (198, 19.9), $\text{H}_3\text{C-C}_6\text{H}_4\text{-O-C}_6\text{H}_4\text{-C}_2\text{H}_5^+$ (212, 20.2), $\text{H}_3\text{C-C}_6\text{H}_4\text{-O-C}_6\text{H}_4\text{-C}_2\text{H}_5^+$ (210, 21.0)
Carbonate	$\text{C}_6\text{H}_5\text{-O-C(=O)-O-C}_6\text{H}_5^+$ (214, 20.4), $\text{C}_6\text{H}_5\text{-O-C(=O)-O-C}_6\text{H}_4\text{-CH}_3^+$ (228, 21.8), $\text{C}_6\text{H}_5\text{-O-C(=O)-O-C}_6\text{H}_3\text{(CH}_3)_2^+$ (242, 23.0), $\text{H}_3\text{C-C}_6\text{H}_4\text{-O-C(=O)-O-C}_6\text{H}_4\text{-CH}_3^+$ (242, 23.2), $\text{C}_6\text{H}_5\text{-O-C(=O)-O-C}_6\text{H}_4\text{-C}_2\text{H}_5^+$ (256, 23.6), $\text{C}_2\text{H}_5\text{-C}_6\text{H}_4\text{-O-C(=O)-O-C}_6\text{H}_4\text{-CH}_3^+$ (256, 24.3), $\text{H}_3\text{C-C}_6\text{H}_4\text{-O-C(=O)-O-C}_6\text{H}_4\text{-C}_2\text{H}_5^+$ (254, 24.5), $\text{H}_3\text{C-C}_6\text{H}_4\text{-O-C(=O)-O-C}_6\text{H}_3\text{(CH}_3)_2^+$ (270, 24.8), $\text{C}_2\text{H}_5\text{-C}_6\text{H}_4\text{-O-C(=O)-O-C}_6\text{H}_4\text{-C}_2\text{H}_5^+$ (268, 25.2), $\text{C}_2\text{H}_5\text{-C}_6\text{H}_4\text{-O-C(=O)-O-C}_6\text{H}_4\text{-C}_2\text{H}_5^+$ (270, 26.2), $\text{C}_2\text{H}_5\text{-C}_6\text{H}_4\text{-O-C(=O)-O-C}_6\text{H}_3\text{(CH}_3)_2^+$ (284, 25.8), $\text{C}_2\text{H}_5\text{-C}_6\text{H}_4\text{-O-C(=O)-O-C}_6\text{H}_4\text{-C}_2\text{H}_5^+$ (282, 26.3), $\text{C}_2\text{H}_5\text{-C}_6\text{H}_4\text{-O-C(=O)-O-C}_6\text{H}_3\text{(CH}_3)_2^+$ (298, 26.5), $\text{C}_2\text{H}_5\text{-C}_6\text{H}_4\text{-O-C(=O)-O-C}_6\text{H}_4\text{-C}_2\text{H}_5^+$ (312, 27.2), $\text{C}_2\text{H}_5\text{-C}_6\text{H}_4\text{-O-C(=O)-O-C}_6\text{H}_3\text{(CH}_3)_2^+$ (326, 28.2),

(\*) Structures confirmed by co-injection.

Table 2. The structures having three benzene rings in GC/MS results

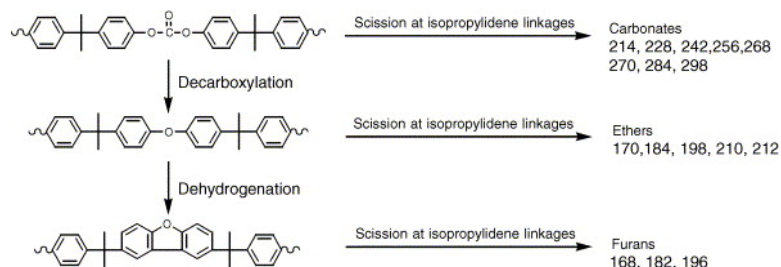
Group	Structures ( <i>m/z</i> , retention time in minutes)
Phosphate	$\text{P(=O)(-OC}_6\text{H}_5)_3^+$ (326, 28.1), $\text{H}_3\text{C-C}_6\text{H}_4\text{-O-P(=O)(-OC}_6\text{H}_5)_2^+$ (340, 29.4), $\text{C}_2\text{H}_5\text{-C}_6\text{H}_4\text{-O-P(=O)(-OC}_6\text{H}_5)_2^+$ (354, 31.1), $\text{HO-C}_6\text{H}_4\text{-O-P(=O)(-OC}_6\text{H}_5)_2^+$ (342, 33.9), $\text{C}_2\text{H}_5\text{-C}_6\text{H}_4\text{-O-P(=O)(-OC}_6\text{H}_4\text{-CH}_3)_2^+$ (352, 31.8), $\text{C}_6\text{H}_5\text{-O-P(=O)(-OC}_6\text{H}_4\text{-CH}_3)_2^+$ (354, 33.0), $\text{P(=O)(-OC}_6\text{H}_4\text{-CH}_3)_3^+$ (368, 35.9), $\text{C}_6\text{H}_5\text{-O-P(=O)(-OC}_6\text{H}_4\text{-CH}_3)_2^+$ (368, 32.2), $\text{C}_6\text{H}_5\text{-O-P(=O)(-OC}_6\text{H}_3\text{(CH}_3)_2)_2^+$ (366, 33.6), $\text{C}_2\text{H}_5\text{-C}_6\text{H}_4\text{-O-P(=O)(-OC}_6\text{H}_4\text{-CH}_3)_2^+$ (382, 32.8), $\text{C}_2\text{H}_5\text{-C}_6\text{H}_4\text{-O-P(=O)(-OC}_6\text{H}_4\text{-CH}_3)_2^+$ (382, 34.7)
Ether	$\text{C}_2\text{H}_5\text{-C}_6\text{H}_4\text{-O-C}_6\text{H}_4\text{-C}_6\text{H}_5^+$ (316, 30.2), $\text{C}_2\text{H}_5\text{-C}_6\text{H}_4\text{-O-C}_6\text{H}_4\text{-C}_6\text{H}_4\text{-OH}^+$ (346, 34.8)
Carbonate	$\text{C}_6\text{H}_5\text{-O-C(=O)-O-C}_6\text{H}_4\text{-C}_6\text{H}_5^+$ (332, 32.3), $\text{H}_3\text{C-C}_6\text{H}_4\text{-O-C(=O)-O-C}_6\text{H}_4\text{-C}_6\text{H}_5^+$ (346, 35.5), $\text{C}_2\text{H}_5\text{-C}_6\text{H}_4\text{-O-C(=O)-O-C}_6\text{H}_4\text{-C}_6\text{H}_5^+$ (360, 38.8), $\text{C}_2\text{H}_5\text{-C}_6\text{H}_4\text{-O-C(=O)-O-C}_6\text{H}_4\text{-C}_6\text{H}_5^+$ (358, 39.9), $\text{C}_2\text{H}_5\text{-C}_6\text{H}_4\text{-O-C(=O)-O-C}_6\text{H}_4\text{-C}_6\text{H}_5^+$ (374, 41.8), $\text{C}_2\text{H}_5\text{-C}_6\text{H}_4\text{-O-C(=O)-O-C}_6\text{H}_4\text{-C}_6\text{H}_5^+$ (372, 44.5), $\text{C}_2\text{H}_5\text{-C}_6\text{H}_4\text{-O-C(=O)-O-C}_6\text{H}_4\text{-C}_6\text{H}_5^+$ (388, 42.9), $\text{C}_6\text{H}_5\text{-O-C(=O)-O-C}_6\text{H}_4\text{-C}_6\text{H}_4\text{-OH}^+$ (348, 43.4), $\text{H}_3\text{C-C}_6\text{H}_4\text{-O-C(=O)-O-C}_6\text{H}_4\text{-C}_6\text{H}_4\text{-OH}^+$ (362, 50.5), $\text{C}_2\text{H}_5\text{-C}_6\text{H}_4\text{-O-C(=O)-O-C}_6\text{H}_4\text{-C}_6\text{H}_4\text{-OH}^+$ (376, 59.6)

(\*) Structures confirmed by co-injection.

The GC traces show that the evolved products for the initial mass loss region consist of mainly TPP (*m/z* 326, 28.1 min retention time), which was confirmed by co-injection, and TPP is observed over the entire mass loss range, even in PC/RDP formulation. This means that some phosphate remains even at very high mass loss, and it

is likely that RDP decomposes to TPP. As the mass loss increases, the intensity of TPP for both formulations decreases and the peaks of the product from PC degradation increase. GC/MS results of PC/phosphate formulations show that many evolved products are the same as those of virgin PC degradation in the main mass loss region [26], [27].

Compared to the degradation results of virgin polycarbonate in air [27], several differences, aside from the peaks pertaining to phosphates, in the GC/MS results are observed in intensity and new compounds. First, the relative intensity of bisphenol A was significantly decreased. Second, the intensities for carbonate compounds and substituted phenols increased. It is notable that many carbonate structures were identified, even diphenylcarbonate ( $m/z$  214, 19.0 min), which was not detected in the degradation of virgin polycarbonate, for both PC/TPP and PC/RDP formulations. Third, some furan compounds, which were not detected in the case of virgin PC degradation, were assigned in the PC/phosphate formulations. It is believed that the furan compounds were produced through the decarboxylation followed by dehydrogenation as shown in Scheme 1; Montaudo et al. suggested a similar pathway for furan formation. The presence of furan in the evolved products implies that some carbonate linkages have undergone reaction prior to evolution. In other words, the phosphate delays the evolution of degraded molecules, and some carbonate linkage may have more opportunity to undergo further reactions, such as dehydrogenation. Scheme 1 shows how the evolved compounds having two benzene rings may be produced. Fourth, structures having unsaturated aliphatic end groups become significant in the presence of phosphates, such as  $m/z$  120 (13.8 min),  $m/z$  134 (15.2 min),  $m/z$  254 (24.5 min) and  $m/z$  268 (25.2 min), which follows the disproportionative dissociation of isopropylidene linkages that was suggested by Montaudo and co-workers [21], [22].



Two compounds, *p*-hydroxybenzaldehyde ( $m/z$  122, 16.2 min) and *p*-hydroxyacetophenone ( $m/z$  136, 17.2 min), which were formed by  $\beta$  scission of alkoxy radicals after peroxide formation in air [27], are observed after the evolution of phosphates.

Fig. 8 shows expanded GC traces for the longer retention time region in the GC/MS and the structures having three benzene rings were assigned, as shown in Table 2; most structures correspond to either phosphates or carbonates. In the case of three benzene ring structures, a relatively small number of ether compounds were assigned, compared to the degradation results of virgin polycarbonate in air. Hence, it can be speculated that the ether-containing group is transformed to either furan or a branched structure in the presence of phosphate.

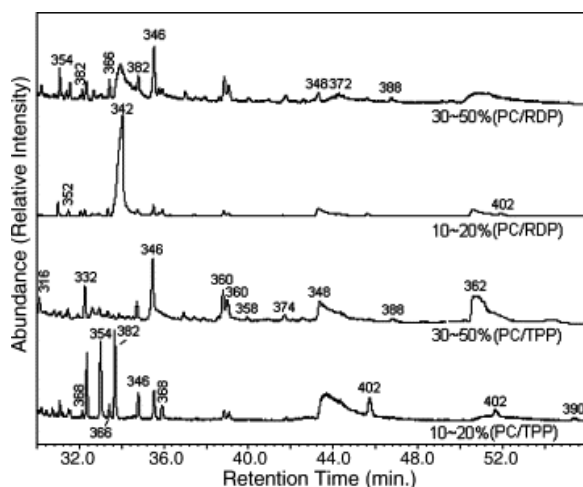
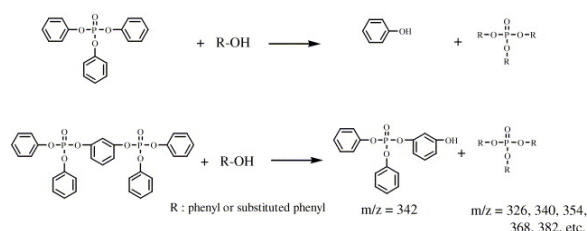
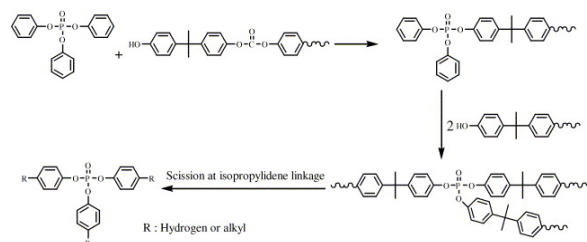


Fig. 8. Expanded GC traces for higher retention time at 10–20 and 30–50% mass loss. Inset numbers indicate the molecular weight acquired by mass spectroscopy. (Data from PC/TPP is an expansion of [Fig. 6](#) while PC/RDP is from [Fig. 7](#).)

The presence of many different phosphates in the evolved products, such as  $m/z$  340 (29.4 min),  $m/z$  342 (33.9 min), etc., implies that an alcoholysis reaction of phosphate has occurred between TPP/RDP and alcohol products evolved from polycarbonate degradation, as shown in [Scheme 2](#), [Scheme 3](#). The assignment of some phosphates, such as  $m/z$  326 (28.1 min),  $m/z$  354 (33.0 min) and  $m/z$  368 (35.9 min), was confirmed by co-injection.



Scheme 2.



Scheme 3.

[Scheme 2](#), [Scheme 3](#) explain why intense peaks due to phenol and alkyl substituted phenol ( $m/z$  94, 108, 122 and 136) were observed in the GC traces and the intensity of bisphenol A ( $m/z$  228, 25.6 min) was reduced in the presence of phosphates ([Fig. 6](#), [Fig. 7](#)). It appears that phosphates may more easily undergo alcoholysis reactions with the alcohol products than does the carbonate linkage of polycarbonate.

It has been proposed that the evolution pathway of bisphenol A is primarily due to the hydrolysis/alcoholysis of the carbonate linkage [\[26\]](#), [\[27\]](#), hence, the carbonate linkage can survive in the presence of phosphate. The reduced intensity of bisphenol A ( $m/z$  228, 25.6 min) and intense carbonates, such as  $m/z$  228 (23.2 min),  $m/z$  242 (23.6 min),  $m/z$  256 (24.3 min), etc., support the notion that the presence of phosphate can stabilize the carbonates from hydrolysis and/or alcoholysis. Even though RDP exhibits less volatility when

compared to TPP, its effects on the degradation of polycarbonate shows characteristics similar to those of TPP, as can be seen from the FTIR and GC/MS results.

The phosphates that have been observed include several structures of aryl-phosphates; mono-alkylphenyldiphenyl phosphates,  $m/z$  340 (29.4 min),  $m/z$  354 (31.1 min),  $m/z$  352 (31.8 min); di-alkylphenylphenyl phosphates,  $m/z$  354 (33.0 min),  $m/z$  366 (33.6 min),  $m/z$  368 (32.2 min); and tri-alkylphenyl phosphates,  $m/z$  368 (35.9 min) and  $m/z$  382 (34.7 min). Thus, it appears that one, two or all three P—O bonds of the phosphate structure may undergo alcoholysis reactions with alcohol products.

### 3.1.3. FTIR analysis of solid residue samples at each temperature

FTIR spectra for the solid residues for both the PC/TPP and PC/RDP formulations as a function of mass loss are shown in Fig. 9, Fig. 10. The FTIR spectra of the solid residues at each mass loss for both PC/TPP and PC/RDP again exhibit similar functionality. The reduction of carbon–hydrogen stretching bands at high mass loss implies carbonization of the residue. In the case of the PC/TPP formulation, the characteristic peak of carbonate,  $1780\text{ cm}^{-1}$ , was observed up to 50% mass loss; in the presence of RDP, the carbonyl peak of carbonate was observed up to 30%.

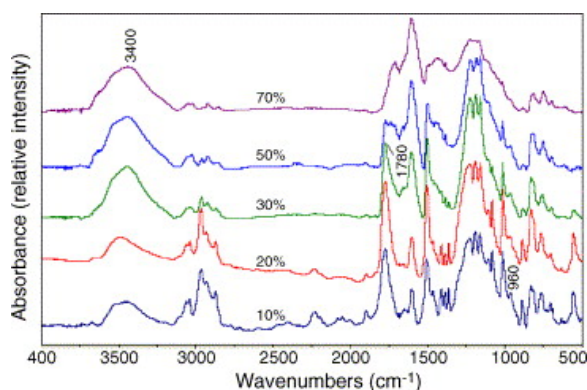


Fig. 9. Condensed phase FTIR for solid residues of PC/TPP at each mass loss in air.

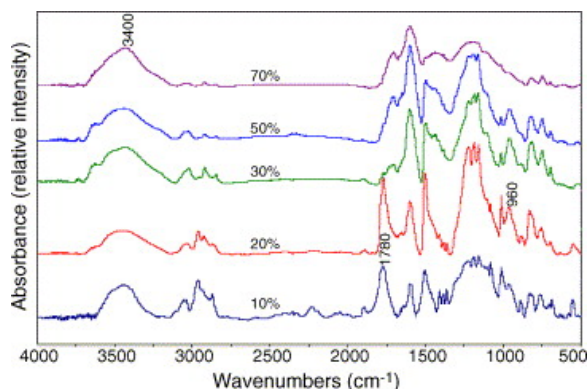


Fig. 10. Condensed phase FTIR for solid residues of PC/RDP at each mass loss in air.

The degradation products containing the alcohol functional group in RDP, such as hydroxyphenyldiphenylphosphate ( $m/z$  342, 33.9 min), shown in Scheme 2, may cause the alcoholysis of the carbonate linkage in the condensed phase of thermally degrading polycarbonate. The band at  $960\text{ cm}^{-1}$ , phosphorus–oxygen stretching, can be observed even at 50% mass loss for both formulations. Since the volatility of RDP is lower than TPP, the intensity of the phosphorus–oxygen stretching in the non-volatile fraction is stronger, which means RDP has greater probability to undergo alcoholysis and form a branched structure.

From the GC/MS results of the evolved products and FTIR of the residues, it is suggested that phosphate in the condensed phase can form branched structures via alcoholysis with the alcohol end groups of degrading

polycarbonate, as shown in [Scheme 3](#). This scheme reflects the presence of phosphate at very high mass loss in the evolved products as well as in the solid residue samples. In the spectra of solid residues at 70% mass loss of PC/TPP and PC/RDP, the phosphate bands disappear. Thus, it is speculated that the branched phosphate structures eventually undergo chain scission at the isopropylidene linkage, producing mono-, di- and tri-substituted phosphates, as shown in [Scheme 3](#).

### 3.2. Flash pyrolysis

In order to simulate real burning behavior, flash pyrolysis at 600 and 800 °C was performed in the TGA instrument for PC, PC/TPP and PC/RDP formulations. [Table 3](#) shows the results on the auto-ignition time and char percentages at each flash temperature. It appears that there is no effect due to phosphate on the auto-ignition time at 800 °C. But, at a temperature of 600 °C, there was no auto-ignition in both PC/TPP and PC/RDP formulation, probably due to the fire retardant effect of the aryl-phosphates. No trend was observed for the effect of phosphate addition on the quantity of char formed after flash pyrolysis.

Table 3. Auto-ignition induction time and char at each flash temperature

Sample	Flash temperature (°C)	Auto-ignition time (s)	Char (%)
PC	800	20	21
	600	75	29
PC/TPP	800	23	18
	600	–	26
PC/RDP	800	23	21
	600	–	30

The concentrations of TPP and RDP are 12 wt.% in their compositions.

The vapor phase FTIR spectra for the volatile products of PC, PC/TPP and PC/RDP during flash pyrolysis are shown in [Fig. 11](#). The FTIR results for flash pyrolysis are qualitatively identical to those of gradual pyrolysis, which means a similar functionality of the evolved products during decomposition. For all formulations,  $sp^2$  carbon–hydrogen stretching bands, above  $3000\text{ cm}^{-1}$ , become more intense at a flash temperature of 800 °C and free alcohol bands at  $3650\text{ cm}^{-1}$  decrease, as compared to gradual pyrolysis. The weak intensity at  $3650\text{ cm}^{-1}$  is due to the decrease of bisphenol A evolution under flash pyrolysis conditions, as will also be seen in the GC/MS results of [Fig. 13](#) and [Table 4](#). The strong band at  $3060\text{ cm}^{-1}$  is due to polynuclear aromatic hydrocarbons, such as naphthalene and phenanthrene [\[30\]](#). It was reported that the evolution of polynuclear aromatic hydrocarbons during combustion was increased as the temperature was increased [\[31, 32\]](#).

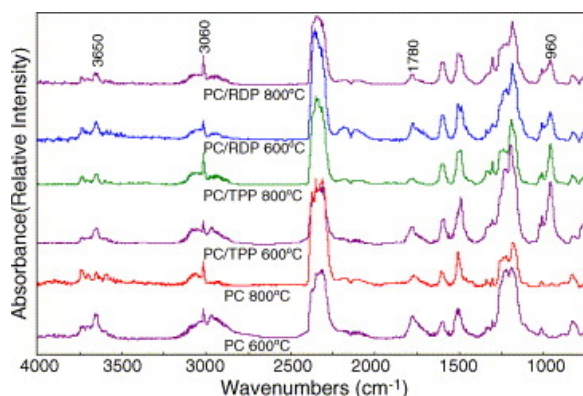
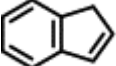
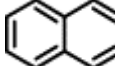
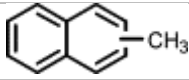
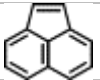
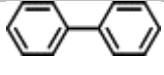
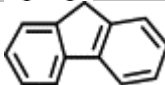
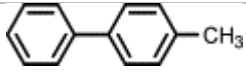
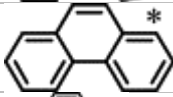
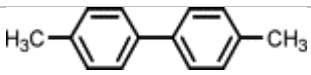
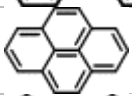
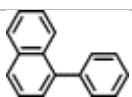
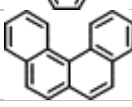


Fig. 11. Vapor phase FTIR of PC, PC/TPP, PC/RDP for the volatile evolved products during flash pyrolysis.

Table 4. The evolved polynuclear aromatic compounds in the flash pyrolysis condition

$m/z$	Retention time (min)	Structure	$m/z$	Retention time (min)	Structure
116	11.0	 *	128	13.5	 *

142	15.4		152	17.7	
154	15.7		166	19.5	
168	18.6		178	21.9	
182	18.9		202	25.1	
204	24.1		228	29.8	

(\*) Structures confirmed by co-injection.

[Fig. 12](#) shows the condensed phase FTIR spectra for the products collected during the flash pyrolysis of PC, PC/TPP and PC/RDP at each temperature. The characteristic carbonate band in the region 1750–1780  $\text{cm}^{-1}$  is observed for all samples. These carbonate bands are more intense at 600 °C in the presence of phosphate than in virgin polycarbonate. At 800 °C, under flash pyrolysis conditions, there is no difference between polycarbonate and PC/phosphate blends in the intensity of carbonyl bands. This trend may be related to the auto-ignition induction time data at 800 °C in [Table 3](#).

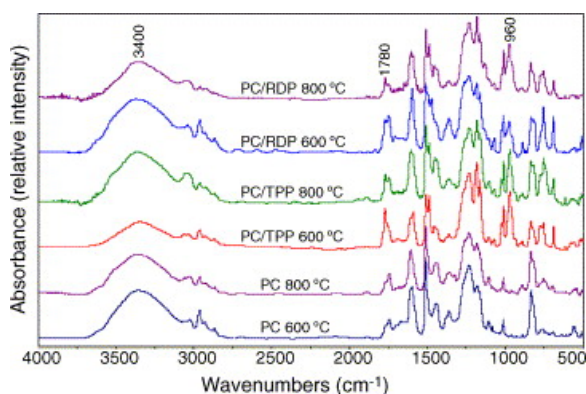


[Fig. 12](#). Condensed phase FTIR of PC, PC/TPP and PC/RDP for the condensable evolved product during flash pyrolysis.

The GC traces of the condensable products for PC, PC/TPP and PC/RDP at each flash temperature are shown in [Fig. 13](#), and have appended to each trace the molecular masses. The molecular structures for each  $m/z$ , which are the same as for the gradual pyrolysis results, were listed in [Table 1](#), [Table 2](#).

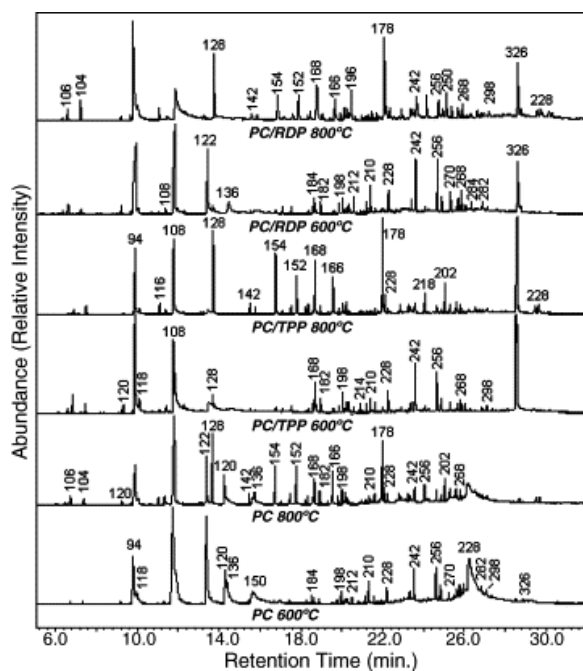


Fig. 13. GC traces of the condensable evolved products of PC, PC/TPP and PC/RDP for flash pyrolysis. Inset number denotes  $m/z$  acquired by mass spectroscopy.

In the case of flash pyrolysis of virgin polycarbonate, the spectrum at a flash temperature of 600 °C is similar to the results for the gradual pyrolysis, except the peak of bisphenol A ( $m/z$  228, 26.1 min) is decreased. This trend becomes more significant at higher flash temperatures. This implies that, in flash pyrolysis, chain scission of the weak bonds may become the dominant degradation pathway for both the isopropylidene and the carbonate linkage of polycarbonate, in agreement with the bond dissociation energies, shown in Fig. 14, rather than the hydrolysis/alcoholysis. Bond dissociation energies indicate the strength of a covalent bond between two atoms. In the degradation study of virgin polycarbonate, it has been shown that the methyl group of isopropylidene linkage undergoes scission first, because the bond energy of this carbon–carbon bond is the smallest, while the carbonate linkage does not follow the bond dissociation energies, because it easily reacts via hydrolysis/alcoholysis. Under flash pyrolysis conditions, the evolution of bisphenol A decreases, which also occurs under gradual pyrolysis conditions in the presence of phosphate. Thus, in this case, the degradation rate is so rapid that the degradation pathway occurs mainly by chain scission of the weak bonds (Fig. 14).

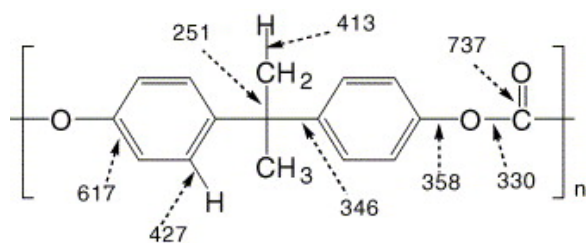


Fig. 14. Bond dissociation energy of bisphenol A polycarbonate in kJ/mol [14], [33].

Polynuclear aromatic hydrocarbons, such as naphthalene ( $m/z$  128, 13.5 min) and phenanthrene ( $m/z$  178, 21.9 min), become significant at a flash temperature of 800 °C. New peaks from the spectra of gradual pyrolysis were assigned according to their mass fragment pattern. The assignments of naphthalene and phenanthrene were confirmed by co-injection. The new peaks observed in flash pyrolysis were identified as polynuclear aromatic compounds as shown in Table 4, which is consistent with FTIR spectra. It was reported that polynuclear aromatic hydrocarbons were formed through sequential hydrogen abstraction and acetylene addition and grow by reactive coagulation of smaller polynuclear aromatic hydrocarbons at very high temperature during

combustion of the polymer [34], [35], [36]. Considerable amounts of soot were formed, along with other typical polynuclear aromatic compounds, during flash pyrolysis of polycarbonate. Higher molecular weight polynuclear aromatic hydrocarbons, larger than benzophenanthrene ( $m/z$  228, 29.8 min), may also be evolved in the flash pyrolysis, probably as soot.

The GC/MS data for the PC/TPP and PC/RDP formulations show the same trends as virgin polycarbonate. As the flash temperature increases to 800 °C, the evolution of polynuclear aromatic hydrocarbons increases. Comparing the GC traces of PC/TPP and PC/RDP with virgin polycarbonate in Fig. 13, some differences are observed in terms of the relative intensity of the evolved products; the phenol peak ( $m/z$  94, 9.5 min) increases, probably due to alcoholysis of phosphates as described in the Scheme 2, Scheme 3, the peaks of *p*-ethylphenol ( $m/z$  122), *p*-propylphenol ( $m/z$  136) and *p*-ethenylphenol ( $m/z$  120) decrease significantly and the intensities of polynuclear aromatic hydrocarbons become more intense in the presence of phosphates. Comparing the GC traces of PC, PC/TPP and PC/RDP at 800 °C, the peaks of *p*-ethylphenol and *p*-propyl phenol disappear in the presence of phosphate, which implies that poly-aromatization of alkyl substituents of benzene ring may be accelerated in the presence of phosphates. This result also suggests that a substituted phenol has more opportunity to undergo poly-aromatization than phenol, which is in agreement with the accepted mechanism for the formation of polynuclear aromatic hydrocarbon [34], [35], [36].

It is notable that the evolution of bisphenol A is not observed for both PC/TPP and PC/RDP, while the bis(alkylphenyl)carbonates, such as  $m/z$  242 (23.6 min) and 256 (24.5 min), are detected in considerable amounts. In the case of flash pyrolysis of virgin PC, one of the abundant compounds is bisphenol A, as is also the case for gradual pyrolysis. In flash pyrolysis, it is thought that the heat supply to the polymer substrate is so large that the degradation rate is very fast, thus the evolution of water and alcohols from polycarbonate degradation does not influence the reactivity of the carbonate group and, hence, the possibility of hydrolysis or alcoholysis of the carbonate group decreases, which suggests that the degradation pathway of polycarbonate is homolytic chain scission along the weak bonds.

The FTIR spectra for the solid residues for PC, PC/TPP and PC/RDP formulation at each temperature are shown in Fig. 15. The diagnostic band of phosphate,  $960\text{ cm}^{-1}$ , is observed at 600 °C with a very small intensity and then disappears in the solid residues at 800 °C. This result shows that the phosphates in PC/aryl-phosphate blend eventually evaporate at high temperature. The FTIR spectra of PC/TPP and PC/RDP solid residues at 800 °C exhibit more a graphite-like structure than does virgin PC. Elemental analysis of the residue at 800 °C shows that a negligible amount of phosphorus is present. Phosphorus was also not detected in the residues at 700 °C in gradual pyrolysis.

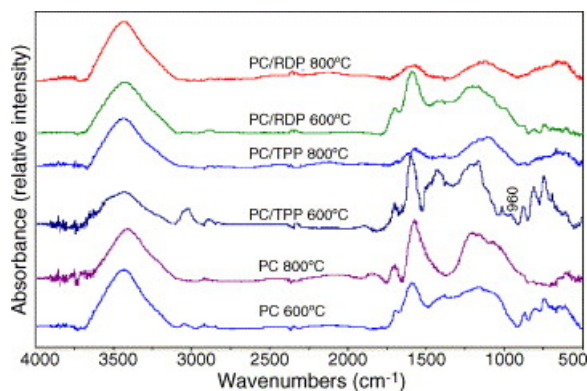


Fig. 15. Condensed Phase FTIR of the solid residue of PC, PC/TPP and PC/RDP.

### 3.3. Role of phosphate and fire retardant action

In this study, it was confirmed that both TPP and RDP stabilize polycarbonate and delay the degradation of polycarbonate and some of the phosphate undergoes alcoholysis reaction with alcohol products that are



evolved during thermal degradation. It appears that the alcoholysis reaction between phosphate and alcohol products is more favorable than the reaction between the carbonate linkage and alcohols. As a result, the evolution of bisphenol A is significantly reduced and diaryl-carbonates increase in the presence of phosphate. A considerable amount of phosphate evolves in the initial mass loss region and some phosphate undergoes alcoholysis with alcohol products and can form branched structures, as shown in [Scheme 3](#). Through this scheme, phosphate can be present up to high mass loss. Besides, these branched phosphate structures may act as a thermal barrier, reduce the fuel production, and help to form more polynuclear aromatic compounds. However, most of the phosphate eventually evolves during thermal degradation and no significant char enhancement at 700 °C was observed using phosphate, which implies that vapor phase fire retardant action is the main mechanism for the phosphate fire retardants. Hence, there is not a significant contribution of phosphate to the final char amount. The difference between RDP and TPP is not significant in terms of the functionality and composition in the evolved products; thus, their fire retardant action is qualitatively the same.

If phosphates are used in non-charring polymers, such as ABS and HIPS, a large amount of phosphate should be added to the polymer composition to obtain a UL 94 V-0 rating. In this case, since these polymers do not produce char upon combustion, it can be considered that gas phase action is the main fire retardant mechanism. While, if phosphates are used with char forming polymers such as PC and PPO, the required amount of phosphate fire retardant for UL94 V-0 rating is significantly reduced. This result may be considered as a synergistic fire retardant effect between fire retardant and the degraded products.

Therefore, very effective fire retardancy arises when phosphates are used with polymers that produce alcohols during thermal degradation, such as polycarbonate, polyphenyleneoxide, polyester, polyurethane, etc., because they may form branched phosphate structures during thermal degradation via alcoholysis, which are available for further reaction.

## 4. Conclusion

Through the analysis of the evolved products and solid residues during thermal degradation of PC, PC/TPP and PC/RDP, it was shown that a considerable amount of TPP and RDP, especially TPP, evaporates in the beginning mass loss region and some undergoes alcoholysis reaction more readily with the alcohol products decomposed from PC than does the carbonate linkage of polycarbonate. Hence, the evolution of bisphenol A, which is mainly produced by the alcoholysis of carbonate linkage, is significantly reduced and the relative intensity diarylcarbonate increases in the presence of phosphate. Thus, the degradation pathway of polycarbonate in the presence of phosphate is primarily the chain scission in weak bonds in terms of the bond dissociation energy. Through alcoholysis between phosphate and the alcohols from polycarbonate degradation, phosphates can form branched structures with the polycarbonate chain, which probably acts as a barrier for heat and mass transfer of the degraded products. It appears that there is no significant difference between TPP and RDP in terms of functionality and the composition of the evolved products and TPP is observed in significant amounts when PC/RDP is pyrolyzed. In the flash pyrolysis study, it was shown that a relatively large amount of polynuclear aromatic hydrocarbons was produced in the presence of phosphate.

## References

- [1] J. Green. A.F. Grand, C.A. Wilkie (Eds.), *Fire Retardancy of Polymeric Materials*, Marcel Dekker, New York (2000) (Chapter 5)
- [2] G.L. Nelson, Fire, I.I. Polymers, G.L. Nelson (Eds.), *ACS Symposium Series 599* (1995), p. 579
- [3] J. Green. *J. Fire Sci.*, 9 (1991), p. 285
- [4] J. Green. *J. Fire Sci.*, 12 (1994), p. 388
- [5] A. Granzow. *Acc. Chem. Res.*, 11 (1978), p. 177
- [6] S.K. Brauman. *J. Fire Ret. Chem.*, 4 (1977), p. 18
- [7] S.K. Brauman, N. Fishman. *J. Fire Ret. Chem.*, 4 (1977), p. 93
- [8] E.D. Weil. R. Engel (Ed.), *Handbook of Organophosphorus Chemistry*, Marcel Dekker (1992), p. 683

- [9] J. Carnahan, W. Haaf, G. Nelson, G. Lee, V. Abolins, P. Shank. *Proceedings of the International Conference on Fire Safety*, vol. 4 (1979), p. 312
- [10] E.A. Murashko, G.F. Levchik, S.V. Levchik, D.A. Bright, S. Dashevsky. *J. Fire Sci.*, 19 (1998), p. 278
- [11] E.A. Murashko, G.F. Levchik, S.V. Levchik, D.A. Bright, S. Dashevsky. *J. Appl. Polym. Sci.*, 71 (1998), p. 1863
- [12] E.A. Murashko, G.F. Levchik, S.V. Levchik, D.A. Bright, S. Dashevsky. *J. Fire Sci.*, 16 (1998), p. 233
- [13] D.W. van Krevelen. *Polymer*, 16 (1975), p. 615
- [14] L.H. Lee. *J. Polym. Sci.*, 2 (1964), p. 2859
- [15] I.C. McNeill, A. Rincon. *Polym. Degrad. Stab.*, 39 (1993), p. 13
- [16] I.C. McNeill, A. Rincon. *Polym. Degrad. Stab.*, 31 (1991), p. 163
- [17] A. Davis, J.H. Golden. *J. Gas Chromatogr.*, 5 (1967), p. 81
- [18] A. Davis, J.H. Golden. *Macromol. Chem.*, 110 (1967), p. 180
- [19] A. Ballistreri, G. Montaudo, C. Puglisi, E. Scamporrino, D. Vitalini, S. Cucinella. *J. Polym. Sci., Polym. Chem. Ed.*, 26 (1988), p. 2113
- [20] G. Montaudo, C. Puglisi. *Polym. Degrad. Stab.*, 37 (1992), p. 91
- [21] C. Puglisi, F. Samperi, S. Carroccio, G. Montaudo. *Macromolecules*, 32 (1999), p. 8821
- [22] C. Puglisi, L. Sturiale, G. Montaudo. *Macromolecules*, 32 (1999), p. 2194
- [23] G. Montaudo, S. Carroccio, C. Puglisi. *Polym. Degrad. Stab.*, 77 (2002), p. 137
- [24] G. Montaudo, S. Carroccio, C. Puglisi. *J. Anal. Appl. Pyrolysis*, 64 (2002), p. 229
- [25] S. Carroccio, C. Puglisi, G. Montaudo. *Macromolecules*, 35 (2002), p. 4297
- [26] B.N. Jang, C.A. Wilkie. *Polym. Degrad. Stab.*, 86 (2004), pp. 419-430
- [27] B.N. Jang, C.A. Wilkie. *Thermochim. Acta*, 426 (2005), pp. 73-84
- [28] A.S. Politou, C. Morterra, M.J.D. Low. *Carbon*, 28 (1990), p. 529
- [29] G. Socrates ***Infrared and Raman Characteristic Group Frequencies***. (third ed.), John Wiley & Sons Ltd. (2001). pp. 117–119
- [30] C.J. Pouchert. *The Aldrich Library of FT-IR Spectra*, 3 (1985), p. 877, 886
- [31] J. Wang, Y.A. Levendis, H. Richter, J.B. Howard, J. Carlson. *Environ. Sci. Technol.*, 35 (2001), p. 3541
- [32] J. Wang, H. Richter, J.B. Howard, Y.A. Levendis, J. Carlson. *Environ. Sci. Technol.*, 36 (2002), p. 797
- [33] X. Li, M. Huang. *Polym. Int.*, 48 (1999), p. 387
- [34] H. Richer, J.B. Howard. *Prog. Energy Combust. Sci.*, 26 (2000), p. 565
- [35] M. Frenklach, D.W. Clary, W.C. Cardinner, S.E. Stein. *Proceedings of the Combustion Institute*, vol. 20 (1984), p. 887
- [36] M. Frenklach. *Phys. Chem. Chem. Phys.*, 4 (2002), p. 2028